18th IEEE International Conference on Control Applications
Part of 2009 IEEE Multi-conference on Systems and Control
Saint Petersburg, Russia, July 8-10, 2009

Robust STATCOM Control for the Enhancement of Fault Ride-Through Capability of Fixed Speed Wind Generators

M. J. Hossain, H. R. Pota, V. Ugrinovskii, Senior Member, IEEE and Rodrigo A. Ramos, Senior Member, IEEE

***Abstract*— In this paper, a novel robust controller for a Static Synchronous Compensator (STATCOM) is presented to enhance the fault ride-through (FRT) capability of fixed speed induction generators (FSIGs), the most common type of generators that can be found in wind farms. The effects of STATCOM rating and wind farm integration on FRT capability of FSIGs are studied analytically using the power-voltage and torque-slip relationships as well as through simulations. The wind generator is a highly nonlinear system, which is modelled in this work as a linear part plus a nonlinear part, the nonlinear term being the Cauchy remainder term in the Taylor series expansion and of the equations used to model the wind farm. Bounds derived for this Cauchy remainder term are used to define an uncertain linear model for which a robust control design is performed. The controller resulting from this robust design provides an acceptable performance over a wide range of conditions needed to operate the wind farm during severe faults. The performance of the designed controller is demonstrated by large disturbance simulations on a test system.**

***Index Terms*— Fault-ride through, STATCOM, Wind Farms, Induction generator, Nonlinearity, Robust Control.**

I. INTRODUCTION

Wind energy has emerged as the fastest growing source of renewable energy and is expected to see continued strong growth in the immediate future. As the total base of installed wind capacity continues to grow with the installation of additional wind turbines and new wind farms, compliance with interconnection criteria becomes increasingly important. Most interconnection standards today require wind farms to have the ability to withstand severe faults, which is usually called Fault Ride-Thorugh (FRT) capability or, in some cases, Low Voltage Ride-Through capability. Typical FRT requirements demand that the wind farm remains connected to the grid for voltage levels as low as 5% of the nominal voltage (for up to 140 ms) [3].

Many of the presently used wind turbines are fixed speed induction generators (FSIGs), which provide a cost effective solution for wind power generation. This type of wind generator always consumes reactive power from the grid. When a disturbance or fault occurs, the voltage at the terminals of the wind turbine drops significantly, causing the electromagnetic torque and electric power output of the generator to be greatly reduced. However, given that the mechanical input torque is almost constant when typical non-permanent faults occur in a wind farm, this leads to an acceleration of the machine rotor. As the slip of the induction generator increases, the reactive power absorbed from the connecting power system increases rapidly. Therefore, unless the turbine is prevented from overspeeding, the voltage on the network is not likely to recover to its pre-fault value when the fault is cleared. After the fault is cleared, a large amount of reactive power is drawn by the generators. If this is not available, the machine will speed out of control and get disconnected from the power system. While the loss of a small capacity wind farm may be acceptable, large wind farms are subjected to Grid Code requirements and must be able to ride through these types of non-permanent disturbances.

Traditionally, switched capacitors have been used to compensate for fluctuating VAr requirements. However, a typical wind farm can experience $50-100$ capacitor switching events on a given day. Such frequent switching can cause stresses, effectively reducing life-cycle times of the capacitor switches. In addition, some wind generator gearboxes are sensitive to large step changes in voltage associated with normal capacitor switching, which can overstress these gearboxes (which are quite costly and require intensive maintenance). Dynamic-VAr systems such as STATCOM with an appropriate controller help meet the wind farm interconnection standards and also provide dynamic voltage regulation, power factor correction, and low voltage ride-through capability for the entire wind farm.

Most literature on STATCOM control, to enhance FRT of fixed speed induction generator, concentrates on control of STATCOM output current and dc bus voltage regulation for a given reactive current reference using a modelling strategy similar to that used for field oriented control of three-phase ac machines [7], [8], [9], [11]. In most of the cases, there are two main control objectives for the converters. One is to regulate the dc term (dc voltage for voltage source converter, and dc current for current-source converter) to a constant value. The other is to control the ac-side reactive power (or power factor). The two loops are designed separately and the interaction is not considered. In addition, the decoupled control of the AC and DC side voltages of STATCOM is difficult to realize due to the inherent coupling between the d-axis and q-axis variables.

This work was supported by the Australian Research Council and the University of New South Wales at the Australian Defence Force Academy (UNSW@ADFA).

M. J. Hossain, H. R. Pota, V. Ugrinovskii are with the school of ITEE, UNSW@ADFA, Canberra, ACT-2600, Australia (m.hossain, h-pota, v.ougrinovski)@adfa.edu.au

R. A. Ramos is with the Dept. of Electrical Engg., Engineering School of São Carlos, Brazil (ramos@sel.eese.usp.br).

The conventional converter model of STATCOM is a multi-input multi-output nonlinear model, and the biggest difficulty in controlling the converters is mainly due to this nonlinear behavior. There are several ways of dealing with nonlinearities. A simple way is to use two PI controllers to control the dc term and the reactive power separately [5]. However, in these cases, the response time is usually long, and it is usually difficult to find appropriate PI parameters in a systematic way. Another method is to linearize the system around an operating point [12] and then design a linear controller. The main problems with this method are due to the facts that the controller looses effectiveness when facing large disturbances and that the design is dependent on the operating point. This motivates the use of advanced control techniques that consider the nonlinear interactions and ensure stability for large disturbances, thus keeping the wind farm connected to the main grid under fault and post-fault conditions.

This paper investigates the stability in power systems with FSIG-based wind farms. The effects of STATCOM rating and increase in wind generation on the FRT capability of the wind farm are analyzed using analytical approximations as well as through detailed simulations. A robust minimax LQG control is designed to control the STATCOM to stabilize the system response to large disturbances. The control approach is to regulate the firing angle α and inverter constant k, which indirectly smooths the electromagnetic torque of induction generators. A linearisation method is used where the Cauchy remainder is included in the design process as a bounded uncertainty. The mean-value theorem allows to retain system nonlinearities in the system model; this improves modelling accuracy of representing nonlinear dynamics. The control design has been tested by nonlinear simulations under various types of large disturbances. The comparison of these results with those obtained from a conventional PI control based STATCOM reveals the efficacy of the proposed STATCOM control design.

The organization of the paper is as follows: Section 2 provides the mathematical modelling of the power system devices under consideration; Section 3 describes the linearisation technique and bounds on nonlinear terms; Section 4 discusses the minimax LQG controller design technique and in Section 5, case studies and the performance of the controller are outlined. Section 6 presents the conclusion.

II. POWER SYSTEM MODEL

A two-mass drive train model of a wind turbine generator system (WTGS) is used in this paper as the drive train modelling can satisfactorily reproduce the dynamic characteristics of WTGS. The dynamics of the shaft are represented as [1]:

$$\dot{\omega}_{wti} = \frac{T_{wti} - K_s\gamma_i}{2H_{wti}}, \quad (1)$$

$$\dot{\omega}_{mi} = \frac{K_{si}\gamma_i - T_{ei}}{2H_{wti}}, \quad (2)$$

$$\dot{\gamma}_i = 2\pi f(\omega_{wti} - \omega_{mi}), \quad (3)$$

where f represents nominal grid frequency, T_i is the torque, γ_i is the angular displacement between the two ends of the shaft, ω_i is the speed, H_i is the inertia constant, and K_{si} is the shaft stiffness. The subscripts wti denote variables related to the ith wind turbine rotor. Similarly, mi and ei denote, respectively, mechanical and electrical variables related to the ith generator.

A simplified transient model of a single cage induction generator with the stator transients neglected and rotor currents eliminated, is described by the following differential equations [1], [10]:

$$\dot{s}_i = \frac{1}{2H_{mi}}\left[T_{mi} - T_{ei}\right], \quad (4)$$

$$\dot{E}'_{qri} = -\frac{1}{T'_{oi}}\left[E'_{qri} - (X_i - X'_i)i_{dsi}\right] - s_i\omega_s E'_{dri}, \quad (5)$$

$$\dot{E}'_{dri} = -\frac{1}{T'_{oi}}\left[E'_{dri} + (X_i - X'_i)i_{qsi}\right] + s_i\omega_s E'_{qri}, \quad (6)$$

The symbols carry their standard meanings [1]. The STATCOM model can be described by the following equation:

$$\dot{v}_{dc}(t) = -\frac{P_s}{Cv_{dc}} - \frac{v_{dc}}{R_cC}, \quad (7)$$

where v_{dc} is the capacitor voltage, $k = \sqrt{(\frac{3}{8})}m$ is a constant associated with the inverter, m is the modulation index, P_s ($P_s = f(\alpha, k, v_t, v_{dc}, E'_{qr}, E'_{dr}, v_t = kv_{dc}\angle\alpha)$, is the power supplied to the STATCOM to charge the capacitor and the control inputs are related to v_{dc} through P_s.

A. Critical clearing time (CCT) and critical voltage

The critical clearing time can be calculated from the induction generator equation

$$\dot{s} = \frac{1}{2H}\left[T_m - T_e\right]. \quad (8)$$

During a solid, three-phase short circuit at the generator terminals we have $T_e = 0$, and then (8) can be written as

$$\dot{s} = \frac{1}{2H}T_m. \quad (9)$$

Integrating both sides

$$s = \int_0^t \frac{1}{2H}T_m + s_0. \quad (10)$$

If s_c is the critical slip of a machine, then the critical clearing time can be given as

$$t_c = \frac{1}{T_m}2H_m(s_c - s_0). \quad (11)$$

The critical speed is given by the intersection between the torque-speed curve for the specified system and the mechanical torque [2]. The critical voltage can be obtained from PV curves [4]. From the power flow equations the relation between voltage and power is given by

$$V = \sqrt{\frac{E^2}{2} - QX \pm \sqrt{\frac{E^4}{4} - X^2P^2 - XE^2Q}}, \quad (12)$$

where the symbols carry their usual meanings. Equations (11) and (12) are solved to estimate the critical clearing time and critical voltage of induction generators.

B. Test System

The test system shown in Fig. 1 consists of two main buses connected via two long parallel transmission lines. Wind turbines are connected to the first bus via transformers and the other bus is connected to the grid. Each induction generator works at the rated operating point and supplies 2 MW of active power. The data for the wind generator is given [1]. We use an aggregated model of the wind farm to design the proposed controller. The load is modelled as a constant impedance load. The wind farm, rated at 50 MW, is not allowed to operate under severe fault conditions and the addition of the STATCOM with appropriate control is expected to increase the stability margin as well as FRT capability of the wind farm.

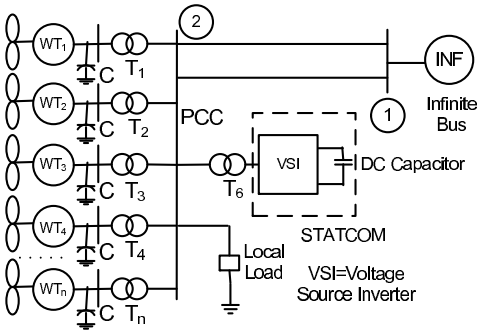

Fig. 1. Power System Model.

III. LINEARISATION AND UNCERTAINTY MODELLING

Conventionally a linear controller is designed based on the Taylor series around an equilibrium point by neglecting the higher order terms. In this paper, to quantify the neglected higher order terms, we propose the use of a linearisation scheme which retains the contributions of the higher order terms in the form of the Cauchy remainder. Let (x_0,u_0) be an arbitrary point in the control space, using mean-value theorem , the system (1)–(7) can be rewritten as follows [6]

$$\dot{x} = f(x_0,u_{i0}) + L(x-x_0) + M(u-u_0), \tag{13}$$

where

$$L = \left[\left.\frac{\partial f_1}{\partial x}\right|_{\substack{x=x^{*1}\\u=u*1}}, \ldots, \left.\frac{\partial f_7}{\partial x}\right|_{\substack{x=x^{*7}\\u=u*7}} \right]^T,$$

$$M = \left[\left.\frac{\partial f_1}{\partial u}\right|_{\substack{x=x^{*1}\\u=u*1}}, \ldots, \left.\frac{\partial f_7}{\partial u}\right|_{\substack{x=x^{*7}\\u=u*7}} \right]^T, \quad f = [f_1,\ldots,f_7]^T.$$

where (x^{*p},u^{*p}) , $p = 1,\cdots,7$, denote points lying in the line segment connecting (x,u) and (x_0,u_0) and f denotes the vector function on the right-hand side of the vector differential equation (1)–(7).

Letting (x_0,u_0) be the equilibrium point about which the trajectory is to be stabilized and defining $\Delta x \triangleq x - x_0$ and $\Delta u \triangleq u - u_0$, it is possible to rewrite (13) as follows

$$\begin{aligned} \Delta\dot{x} &= \dot{x} - \dot{x_0}, \\ &= A\triangle x + (L-A)\triangle x + B_1\triangle u, \end{aligned} \tag{14}$$

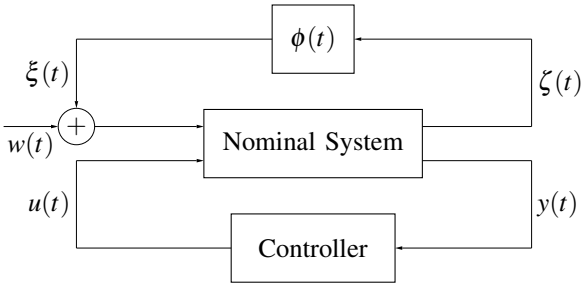

Fig. 2. Uncertain System

where $A = \frac{\partial f}{\partial x}|_{\substack{x=x_0\\u=u_0}}$, $B_1 = \frac{\partial f}{\partial u}|_{\substack{x=x_0\\u=u_0}}$, $u = [k,\alpha]$ and $\triangle x = [\triangle s, \triangle E_{dr}, \triangle E_{qr}, \triangle\omega_{wt}, \triangle\omega_m, \triangle\gamma, \triangle V_{dc}]^T$. Since $x^{*p}, p = 1,\ldots,7$ are not known, it is difficult to obtain the exact value of $(L-A)$, but it is possible to obtain a bound on $\|(L-A)\|$. We rewrite system (14) in terms of the block diagram shown in Fig. 2. Let

$$(L-A)\triangle x + (M-B_1)\triangle u = B_2\xi(t), \tag{15}$$

where $\xi(t)$ is known as the uncertainty input. Matrices B_2 and C_1 are chosen such that

$$B_2 = \text{diag}\left(\frac{1}{2H_m}, \frac{X_s-X_s'}{T_0'}, \frac{X_s-X_s'}{T_0'}, 0, \frac{1}{2H_{wt}}, 0, \frac{1}{C}\right),$$

$$C_1 = \begin{bmatrix} 1&0&0&0&0&0&0\\ 0&1&0&0&0&0&0\\ 0&0&1&0&0&0&0\\ 0&0&0&0&0&0&1 \end{bmatrix}, \quad \tilde{D}_1 = \begin{bmatrix} 1&1\\ 1&1\\ 1&1\\ 1&1 \end{bmatrix}, \tag{16}$$

$$\begin{aligned} &(L-A)\triangle x + (M-B_1)\triangle u = \\ &\quad B_2\tilde{\phi}(t)\tilde{C}_1\triangle x + B_2\tilde{\psi}(t)\tilde{D}_1\triangle u \end{aligned} \tag{17}$$

The expressions for obtaining $\tilde{\phi}(t)$ and $\tilde{\psi}(t)$ are given in Appendix-I.

The system can now be written as

$$\triangle\dot{x} = A\triangle x + B_1\triangle u + B_2\xi(t). \tag{18}$$

Next we introduce a scaling parameter β and write $C_1 = \sqrt{\beta}\tilde{C}_1$, and $D_1 = \sqrt{\beta}\tilde{D}_1$, where β is a scaling factor which affect the magnitude of the uncertain output ζ and

$$\zeta = \sqrt{\beta}\left(\tilde{C}_1\triangle x + \tilde{D}_1\triangle u\right). \tag{19}$$

We write $\phi(t) = \frac{1}{\sqrt{\beta}}\begin{bmatrix}\tilde{\phi}(t) & \tilde{\psi}(t)\end{bmatrix}$. Finally the value of β is chosen such that the uncertainty, $\phi(t)$, shown in Fig. 2 satisfies,

$$\|\phi(t)\|^2 \le 1. \tag{20}$$

From this, we have

$$\|\xi(t)\|^2 \le \beta\|\left(\tilde{C}_1\triangle x + \tilde{D}_1\triangle u\right)\|^2. \tag{21}$$

and we recover the IQC (integral quadratic constraint) given in [13],

$$\|\xi(t)\|^2 \le \|\zeta(t)\|^2. \tag{22}$$

To facilitate control design, the power system model is finally summarized as

$$\triangle \dot{x}(t) = A\triangle x(t) + B_1 \triangle u(t) + B_2 \xi(t) = B_2 w(t), \quad (23)$$

$$y(t) = C_2 \triangle x(t) + D_2 \xi(t)), \quad (24)$$

$$\zeta(t) = C_1 \triangle x(t) + D_1 u(t), \quad (25)$$

where ζ is known as the uncertainty output, $y(t)$ is the measured output, and $w(t)$ is a unity covariance Gaussian white noise process corresponding to the nominal disturbance. The output matrix is defined as $C_2 = \left[1,0,0,0,0,0,0,0\right]$. Equations(23)-(25) provide a new representation of the power system model which contains the linear part , and also another part with higher order terms. The new formulation presented in this section is used with the minimax LQG control theory to design a STATCOM controller for the nonlinear wind generator.

IV. MINIMAX LQG STATCOM CONTROL

The minimax LQG method is applied to the uncertain systems of the form shown in Fig. 2. Associated with the uncertain system (23)–(25), we consider a cost functional J of the form

$$J = \lim_{T\to\infty} \frac{1}{2T} E \int_0^T (x(t)^T R x(t) + u(t)^T G u(t)) dt, \quad (26)$$

where $R \geq 0$ and $G > 0$, $R \in R^{n\times n}, G \in R^{m\times m}$ and E is the expectation.

The minimax optimal control problem can be rewritten in the following form [13]:

$$\sup_{\|\xi\|^2 \leq \|\zeta\|^2} J(u^*) \leq \inf_{\tau} V_\tau, \quad (27)$$

where V_τ is given by

$$V_\tau = \frac{1}{2}\mathrm{tr}[Y_\infty R_\tau + (Y_\infty C_2^T + B_2 D_2^T)(D_2 D_2^T)^{-1} \times (C_2 Y_\infty + D_2 B_2^T) X_\infty (I - \frac{1}{\tau} Y_\infty X_\infty)^{-1}], \quad (28)$$

τ is a free parameter and the matrices X_∞ and Y_∞ are the solution to the following pair of parameter dependent algebraic Riccati equations [13]:

$$(A - B_2 D_2^T (D_2 D_2^T)^{-1} C_2) Y_\infty + Y_\infty (A - B_2 D_2^T \times (D_2 D_2^T)^{-1} C_2)^T - Y_\infty (C_2^T (D_2 D_2^T)^{-1} C_2 - \frac{1}{\tau} R_\tau) Y_\infty + B_2 (I - D_2^T (D_2 D_2^T)^{-1} D_2) B_2^T = 0, \quad (29)$$

and

$$X_\infty (A - B_1 G_\tau^{-1} \gamma_\tau^T + (A - B_1 G_\tau^{-1} \gamma_\tau^T) X_\infty + (R_\tau - \gamma_\tau G_\tau^{-1} \gamma_\tau^T) - X_\infty (B_1 G_\tau^{-1} B_1^T - \frac{1}{\tau} B_2 B_2^T) X_\infty = 0. \quad (30)$$

The solutions are required to satisfy the following conditions: $Y_\infty > 0$, $X_\infty > 0$, the spectral radius of the matrix $X_\infty Y_\infty$ is $\rho(X_\infty Y_\infty) < \tau$, $R_\tau - \gamma_\tau^T G_\tau^{-1} \gamma_\tau \geq 0$, $R_\tau = R + \tau C_1^T C_1$, $G_\tau = G + \tau D_1^T D_1$, $\gamma_\tau = \tau C_1^T D_1$.

To obtain the minimax LQG controller, the parameter $\tau > 0$ is be chosen to minimize the quantity V_τ. A line search is carried out to find the value of $\tau > 0$ which attains the minimum value of the cost function V_τ. This line search involves solving the Riccati equations (29) and (30) for different values of τ and finding that value which gives the smallest V_τ.

TABLE I

EFFECT OF GROWING WIND POWER

Wind Power (MW)	Parameters	Critical speed and CCT from calculation	Critical speed and CCT from simulation
2	ω_{critical}	1.47	1.415
	CCT	0.45	0.485
10	ω_{critical}	1.42	0.137
	CCT	0.40	0.423
20	ω_{critical}	1.37	1.298
	CCT	0.35	0.382
30	ω_{critical}	1.345	1.298
	CCT	0.325	0.344
40	ω_{critical}	1.31	1.295
	CCT	0.29	0.318
50	ω_{critical}	1.285	1.274
	CCT	0.265	0.281

The minimax LQG optimal controller is given by the equations [13]:

$$\dot{\hat{x}}_c = (A - B_1 G_\tau^{-1} \gamma_\tau^T)\hat{x_c} - ((B_1 G_\tau^{-1} B_1^T - \frac{1}{\tau} B_2 B_2^T) X_\infty)\hat{x_c} \times (Y_\infty C_2^T + B_2 D_2^T) + (I - \frac{1}{\tau} Y_\infty X_\infty)^{-1} \times (D_2 D_2^T)^{-1} \left(y - (C_2 + \frac{1}{\tau} D_2 B_2^T X_\infty)\hat{x_c} \right), \quad (31)$$

$$u = -G_\tau^{-1} (B_1^T X_\infty + \gamma_\tau^T)\hat{x_c}. \quad (32)$$

V. CASE STUDIES AND CONTROLLER PERFORMANCE

The FRT capability of wind generator is expressed in this paper as voltage and transient stability margins. The voltage stability margin is defined as the difference between the operating voltage and the critical voltage. The transient stability margin is given as the difference between the speed after a specified fault duration and the critical speed of generator. The pre-fault mechanical torque is 1.0 pu and speed is 1.02 pu. Critical slip and critical clearing time for increasing wind generation are given in Table I. The power-voltage relation for the increasing wind generation is shown in Fig. 3. It can be seen that as the number of wind generators increases, the corresponding critical speed and critical clearing time and terminal voltage decrease. The maximum difference between the estimated value obtained from (11) and that obtained using detailed simulation is 3.74% for critical speed and 7.8% for the CCT. The estimated speed is larger than the values obtained from the detailed simulations. This error is caused by the transients at the time of reclosing, since some time is needed to re-magnetize the induction generator before it is able to output the electrical torque as given by the steady-state speed-torque characteristics.

Critical slip for the different STATCOM MVA ratings, with PI controllers and terminal voltage feedback, are given in Table II. It is observed that the STATCOM significantly increases the critical speed, and thereby the stability limit as

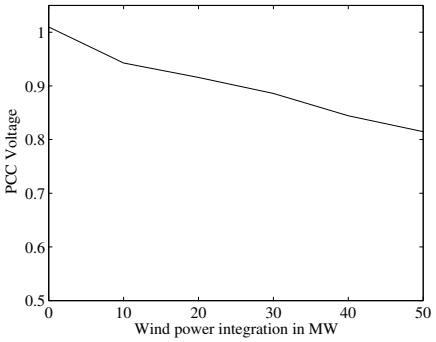

Fig. 3. PV relation at bus PCC

TABLE II
EFFECT OF STATCOM RATINGS

STATCOM (MVA)	Error (s)	Critical speed and CCT from calculation	Critical speed and CCT from simulation
0	ω_{critical}	1.285	1.174
	CCT	0.265	0.281
10	ω_{critical}	1.35	1.28
	CCT	0.315	0.33
25	ω_{critical}	1.40	1.31
	CCT	0.38	0.396
40	ω_{critical}	1.44	1.38
	CCT	0.42	0.437

well as FRT capability of the induction generator, resulting in a corresponding increase of critical clearing time during a three-phase fault. From the data in Table II, it can be concluded that the system with higher rating STATCOM can have longer ride-through times for short-circuit faults.

A. Performance of the Proposed Controller

We carry out several simulations to get an idea about the operating range during transients by applying large disturbances. The controller is designed as follows:

Step 1 From the simulations of the faulted system, obtain the range of the variation of all state variables and form a volume Ω with corner points given by $(x_{f_p} - x_{0_p}), p = 1,\ldots,7$, where x_{f_p} is the largest variation of the p^{th} state variable about its equilibrium value x_{0_p}.

Step 2 Obtain

$$\beta^* = \max_{x^{*p}\in\Omega} \left\{\beta : ||\tilde{\tilde{\psi}}(t)||^2 < 1\right\}.$$

Step 3 Check if there exists a feasible controller with $\beta = \beta^*$, i.e., if there exists a scalar τ such that there is a feasible solution to the coupled Riccati equations (29)–(30).

Step 4 If we obtain a feasible controller in the above step, either enlarge the volume Ω, i.e., increase the range of the controller, or if we have arrived at the largest possible volume then perform an optimal search over the scalar parameter τ to get the infimum of V_τ. If there is no feasible solution with the chosen $\beta = \beta^*$, reduce the volume Ω and go to Step 2. This process enables the selection of the largest range for which a feasible controller is obtained. For the given power system model, we are able to obtain a feasible controller with the value of $\beta = 0.96$ for the range of $|s^* - s_0| = 0.43$, $|E^*_{dr} - E_{dr0}| = 0.29$, $|E^*_{qr} - E_{qr0}| = 0.29$, $|\omega^*_{wt} - \omega_{wt0}| = 0.32$, $|\omega^*_m - \omega_m| = 0.43$, $|\gamma^* - \gamma_0| = 0.21$, $|V^*_{dc} - V_{dc0}| = 0.35$, $|k^* - k_0| = 0.27$, and $|\alpha^* - \alpha_0| = 45^0$.

The performance of the proposed controller for a 10 MVA STATCOM is evaluated for sudden outage of one of the lines serving the wind farm. Outage of one transmission line increases the equivalent line impedance and weakens the interconnection considerably. Due to the increase of the equivalent line reactance, extra reactive power is needed in order to maintain the voltage at the PCC (point of common coupling). The generator speed and terminal voltage with the PI and the proposed STATCOM controller are shown in Figs. 4 and 5.

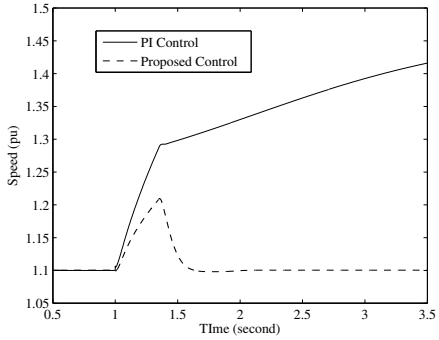

Fig. 4. Speed for the outage of one line.

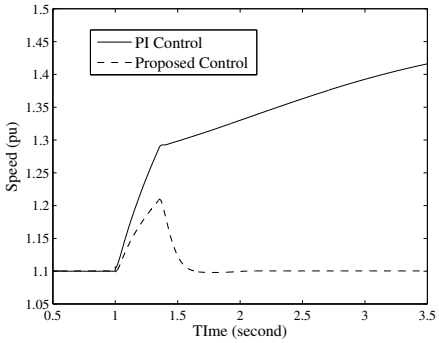

Fig. 5. PCC voltage for the outage of one line.

It is clear that proposed controller can stabilize the voltage as well as induction generator with fault clearing time 0.35s. The speed of 1.32 pu at the fault clearing is greater than the critical speed of 1.28 pu as obtained for the PI controller with numerical simulations. Thus with PI controllers the speed continues to increase even after the fault is cleared. Furthermore, the voltage gradually decreases and the wind generators have to be disconnected from the grid to protect them and avoid voltage collapse.

VI. CONCLUSIONS

This paper has presented effects of the increase in wind generation and STATCOM ratings on FRT capability of a wind farm. It was observed that the critical speed and voltage, as well as the FRT capability, decrease with the integration of FSIGs. On the other hand, the system with a higher rating STATCOM can have a longer FRT capability. Detailed modeling of each component and a suitable control strategy of STATCOM is presented. The STATCOM controller scheme is based on the reformulation of the nonlinear system model using the mean-value theorem. With this new representation, it becomes easier to explicitly account for the effect of nonlinearities in the system dynamics, which enables us to more accurately represent the system and also provide guaranteed performance and stability characteristics over a pre-specified region around an equilibrium point. The performance of the proposed STATCOM controller is compared with a PI-based STATCOM and simulation results confirm the better efficacy of the proposed controller with respect to the conventional STATCOM controller. The designed controller is linear and therefore implementing it should pose no practical difficulties.

APPENDIX I

We define $\tilde{\phi} = \left[\tilde{\phi}_1, \cdots, \tilde{\phi}_7\right]^T$, $\tilde{\psi} = [\tilde{\psi}_1, \cdots, \tilde{\psi}_7]^T$, $z_1 = T_0'/(X-X')$, $z_2 = -\omega_s(E_{qr}^{'*} - E_{qr0}')$, $z_3 = -\omega_s(s^* - s_0)$, $z_4 = \omega_s(E_{dr}^{'*} - E_{dr0}')$, and $\Lambda = (k^* - k_0)$, $v_1 = -(E_{dr}^{*'}V_{dc}^* - E_{dr0}V_{dc0})$, $v_2 = -(E_{qr1}^*V_{dc}^* - E_{qr10}V_{dc0})$ and $z = \frac{1}{V_t^*} - \frac{1}{V_{to}}$ where

$$\tilde{\phi}_1 = \begin{bmatrix} a_{11} \\ a_{12} \\ a_{13} \\ a_{14} \end{bmatrix}^T \begin{bmatrix} 0 & b_{12} & b_{13} & b_{14} \\ 0 & b_{22} & b_{23} & b_{24} \\ 0 & V_\infty G_{13} & V_\infty B_{13} & 0 \\ 0 & V_\infty B_{13} & V_\infty G_{13} & 0 \end{bmatrix} + \begin{bmatrix} 0 \\ c_{12} \\ c_{13} \\ 0 \end{bmatrix}^T,$$

where

$$\begin{aligned}
&a_{11} = \sin(\alpha^* - \delta^*) - \sin(\alpha_0 - \delta_0), a_{13} = -\cos\alpha^* + \cos\alpha_0, \\
&a_{12} = \cos(\alpha^* - \delta^*) - \cos(\alpha_0 - \delta_0), a_{14} = -\sin\alpha^* + \sin\alpha_0, \\
&b_{12} = G_{12}\Lambda(V_{dc}^* - V_{dc0}), b_{22} = -B_{12}\Lambda(V_{dc}^* - V_{dc0}), \\
&b_{13} = -B_{12}\Lambda(V_{dc}^* - V_{dc0}), b_{23} = -G_{12}\Lambda(V_{dc}^* - V_{dc0}) \\
&b_{14} = -\Lambda B_{12}(E_{qr}^{'*} - E_{qr0}') + \Lambda G_{12}(E_{dr}^{'*} - E_{dr0}'), \\
&b_{24} = -\Lambda G_{12}(E_{qr}^{'*} - E_{qr0}') - \Lambda B_{12}(E_{dr}^{'*} - E_{dr0}'), \\
&c_{12} = 2G_{11}(E_{dr}^{'*} - E_{dr0}'), c_{13} = -2B_{11}(E_{qr}^{'*} - E_{qr0}').
\end{aligned}$$

$$\tilde{\phi}_2 = \begin{bmatrix} a_{11} \\ a_{12} \\ a_{13} \\ a_{14} \end{bmatrix}^T \begin{bmatrix} 0 & 0 & 0 & -\Lambda G_{12} \\ 0 & 0 & 0 & \Lambda B_{12} \\ 0 & 0 & 0 & 0 \\ 0 & 0 & 0 & 0 \end{bmatrix} + z_1 \begin{bmatrix} z_2 \\ 0 \\ z_3 \\ 0 \end{bmatrix}^T.$$

$$\tilde{\phi}_3 = \begin{bmatrix} a_{11} \\ a_{12} \\ a_{13} \\ a_{14} \end{bmatrix}^T \begin{bmatrix} 0 & 0 & 0 & \Lambda B_{12} \\ 0 & 0 & 0 & \Lambda G_{12} \\ 0 & 0 & 0 & 0 \\ 0 & 0 & 0 & 0 \end{bmatrix} + z_1 \begin{bmatrix} z_4 \\ z_3 \\ 0 \\ 0 \end{bmatrix}.$$

$$\tilde{\phi}_4 = \tilde{\phi}_6 = [0,0,0,0], \quad \tilde{\phi}_5 = \tilde{\phi}_1,$$

$$\tilde{\phi}_7 = \begin{bmatrix} a_{11} \\ a_{12} \\ a_{13} \\ a_{14} \end{bmatrix} \begin{bmatrix} 0 & -\Lambda B_{12} & -\Lambda G_{21} & 0 \\ 0 & -\Lambda G_{12} & \Lambda B_{21} & 0 \\ 0 & 0 & 0 & 0 \\ 0 & 0 & 0 & 0 \end{bmatrix}$$

$$\tilde{\psi}_1 = \begin{bmatrix} a_{12} & a_{11} \end{bmatrix} \begin{bmatrix} s_{11} & s_{12} \\ s_{21} & s_{22} \end{bmatrix},$$

where

$$\begin{aligned}
&s_{11} = v_1B_{12} + v_2G_{12}, s_{21} = v_1G_{12} + v_2B_{12}, \\
&s_{12} = \Lambda v_1G_{12} - \Lambda v_2B_{12}, s_{22} = -\Lambda v_1B_{12} - \Lambda v_2G_{12}.
\end{aligned}$$

$$\tilde{\psi}_2 = \begin{bmatrix} r_{11} & r_{12} \end{bmatrix} \begin{bmatrix} t_{11} & t_{12} \\ t_{21} & t_{22} \end{bmatrix},$$

where

$$\begin{aligned}
&t_{11} = -(V_{dc}^* - V_{dc0})B_{12}, t_{21} = -(V_{dc}^* - V_{dc0})G_{12}, \\
&t_{12} = -\Lambda(V_{dc}^* - V_{dc0})G_{12}, t_{22} = \Lambda(V_{dc}^* - V_{dc0})B_{14}.
\end{aligned}$$

$$\tilde{\psi}_3 = \begin{bmatrix} r_{11} & r_{12} \end{bmatrix} \begin{bmatrix} u_{11} & u_{12} \\ u_{21} & u_{22} \end{bmatrix},$$

where

$$\begin{aligned}
&u_{11} = -(V_{dc}^* - V_{dc0})G_{12}, u_{21} = (V_{dc}^* - V_{dc0})B_{12}, \\
&u_{12} = \Lambda(V_{dc}^* - V_{dc0})B_{12}, u_{22} = \Lambda(V_{dc}^* - V_{dc0})G_{12}.
\end{aligned}$$

$$\tilde{\psi}_4 = \tilde{\psi}_6 = [0,0], \quad \tilde{\psi}_5 = \tilde{\psi}_1,$$

$$\tilde{\psi}_7 = z \begin{bmatrix} a_{12} & -a_{11} \end{bmatrix} \begin{bmatrix} -s_{12} & -s_{11} \\ -s_{22} & -s_{21} \end{bmatrix}.$$

REFERENCES

[1] T. Ackermann, *Wind Power in Power Systems*. England: John Wiley and Sons, Ltd, 2005.

[2] V. Akhmatov, H. Knudsen, M. Bruntt, A. Nielsen, J. K. Pedersen, and N. K. Poulsen, "A dynamic stability limit of grid-connected induction generator," in *IASTED, International Conference on Power and Energy System*, September 2000, pp. 235–244.

[3] D. Bary, "Increasing renewable accessibility in ireland," in *9th World Energy Congr.*, vol. 1, September 2004, pp. 1–10.

[4] T. V. Cutsem and C. Vournas, *Voltage Stability of Electric Power System*. Norwell, MA: Kluwer Academic, 1998.

[5] R. Itoh and K. lshizaka, "Series connected PWM GTO current/source convertor with symmetrical phase angle control," in *IEE Proceedings*, vol. 137, no. 4, July 1990, pp. 205–212.

[6] H. K. Khalil, *Nonlinear Systems*. Macmillan, New York: Prentice-Hall, 1992.

[7] M. Molinas, J. A. Suul, and T. Undeland, "Wind farms with increased transient stability margin provided by a STATCOM," in *International Conference on Power Electronics and Motion Control Conference, IPEMC '06*, vol. 1, August 2006, pp. 1–7.

[8] ——, "Improved grid interface of induction generators for renewable energy by use of STATCOM," in *International Conference on Clean Electrical Power, ICCEP'07*, May 2007, pp. 215–222.

[9] S. M. Muyeen, M. A. Mannan, M. H. Ali, R. Takahashi, T. Murata, and J. Tamura, "Stabilization of grid connected wind generator by STATCOM," in *International Conference on Power Electronics and Drives Systems, PEDS*, vol. 2, November 2005, pp. 1584–1589.

[10] K. Nandigam and B. H. Chowdhury, "Power flow and stability models for IGs used in wind turbines," in *Power Engineering Society General Meeting, 2004, IEEE*, vol. 2, June 2004, pp. 2012–2016.

[11] L. Qi, J. Langston, and M. Steurer, "Applying a STATCOM for stability improvement to an existing wind farm with fixed-speed induction generators," in *Power and Energy Society General Meeting*, July 2008, pp. 1–6.

[12] C. Shen, Z. Yang, M. L. Crow, and S. Atcitty, "Control of STATCOM with energy storage device," in *IEEE Power Eng. Soc. Winter Meeting Conf.*, January 2000, pp. 2722–2728.

[13] V. A. Ugrinovskii and I. R. Petersen, "Minimax LQG control of stochastic partially observed uncertain systems," *SIAM J. Control Optim.*, vol. 40, no. 4, pp. 1189–1226, 2001.